

Experimental Demonstration of Hydraulic Jump Control in Liquid Metal Channel Flow Using Lorentz Force

A. E. Fisher^a, E. Kolemen and M. G. Hvasta

Princeton University, Dept. of Mechanical & Aerospace Engineering, Princeton, NJ, 08544, USA

Princeton Plasma Physics Laboratory, Princeton, NJ 08543

^aAuthor to whom correspondence should be addressed. E-mail: aefisher@princeton.edu

Abstract: Flowing liquid metals are a proposed solution to heat flux challenges posed in fusion reactors, specifically the tokamak. Thin, fast-flowing liquid metal divertor concepts for fusion reactors are susceptible to hydraulic jumps. Within a tokamak, the occurrence of a hydraulic jump in a fast-flowing, liquid metal plasma facing component (LM-PFC) will drastically reduce flow speed, leading to potential problems such as excessive evaporation, unsteady power removal and possible plasma disruption. Highly electrically conductive flows within magnetic fields do not exhibit traditional hydraulic jump behavior. Additionally, using externally injected electrical currents and the existing toroidal magnetic field inside a tokamak, a Lorentz force (also referred to as $j \times B$ force) may be generated to control the liquid metal jump behavior. In this work, free-surface liquid metal—GalInSn or “galinstan”—flow through an electrically insulating, rectangular duct was investigated. It was shown that applying a Lorentz-force has a repeatable and predictable impact on hydraulic jump that can be used for LM-PFC control in next-generation fusion reactors.

1. Introduction

1.1 Nomenclature

| Var. | Meaning | Units & Constants |
|----------|---|----------------------------|
| u | Flow velocity | [m/s] |
| h | Flow depth (also referred to as height) | [m], [cm], [mm] |
| 0 | Subscript for value upstream of a hydraulic jump | [] |
| 1 | Subscript for value downstream of a hydraulic jump | [] |
| g | Gravitational acceleration | 9.81 [m/s ²] |
| Fr | Froude number upstream of the hydraulic jump | [] |
| Q | Volumetric flow rate | [liter/min] |
| F_L | Lorentz ($j \times B$) force from externally injected electrical currents | [N/m ³] |
| B | Magnetic field | [T] |
| j | Electric current density | [A/m ²] |
| I | Electric current | [A] |
| w | Channel width | 0.109 [m] |
| γ | Ratio of vertical $j \times B$ force to gravitational force | [] |
| ρ | Density of galinstan | 6.4e3 [kg/m ³] |
| μ | Dynamic viscosity of galinstan | 2.4e-3 [Pa s] |
| S | Jump sensitivity | [] |
| F_D | Drag force on liquid metal due to induced electrical currents | [N/m ³] |

1.2 Background

Hydraulic jumps are well-known phenomena found in free-surface supercritical flows where thin, fast flow rapidly changes to thicker, slower flow. Hydraulic jumps have been studied for many applications, with the first studies taking place nearly two hundred years ago [1]. The Froude number is the most important dimensionless parameter that is used to characterize hydraulic jump, and is given in Eq. 1

| | | |
|--|--------------------------------|-------|
| | $Fr = \frac{u_0}{\sqrt{gh_0}}$ | Eq. 1 |
|--|--------------------------------|-------|

A Froude number greater than unity implies that the flow is supercritical. This translates to the average flow velocity being greater than the wave speed allowing for hydraulic jump to occur. There are several types and regimes of hydraulic jump, and the magnitude of the Froude number helps characterize the jump type [2].

Mass and momentum conservation equations are used in order to derive some of the most useful equations for hydraulic jumps. For channels or ducts of constant width, Eq. 2 is used to express conservation of mass in an incompressible flow.

| | | |
|--|-----------------------------|-------|
| | $Q = u_0 h_0 w = u_1 h_1 w$ | Eq. 2 |
|--|-----------------------------|-------|

Ignoring viscous losses and assuming constant duct width, Eq. 3 is used to express momentum conservation. Neglecting viscous and other losses is a reasonable approximation as the hydraulic jump takes place over a relatively short length, causing these losses to be small.

| | | |
|--|---|-------|
| | $\frac{\rho g h_0^2}{2} + \rho u^2 h_0 = \frac{\rho g h_1^2}{2} + \rho u^2 h_1$ | Eq. 3 |
|--|---|-------|

Using Eq. 1 through Eq. 3 with some additional manipulations, the depth change following a hydraulic jump can be derived resulting in the classic relation given in Eq. 4:

| | | |
|--|--|-------|
| | $\frac{h_1}{h_0} = \frac{\sqrt{1 + 8Fr^2} - 1}{2}$ | Eq. 4 |
|--|--|-------|

Hydraulic jumps in traditional flows such as water coming out of a sluice gate have been thoroughly studied. However, hydraulic jumps in flows with added magnetohydrodynamic (MHD) effects are not as well understood. MHD effects result from highly electrically conductive fluids

moving through magnetic fields, and/or from externally injected electrical currents interacting with existing magnetic fields. The interaction between the externally injected electrical currents and magnetic fields creates a Lorentz force (also referred to as a $j \times B$ force from the equation it's defined by). The force manifests as a body force on the flow given by Eq. 5. The electrical current density j here is given by Eq. 6.

| | | |
|--|--------------------|-------|
| | $F_L = j \times B$ | Eq. 5 |
|--|--------------------|-------|

| | | |
|--|--------------------|-------|
| | $j = \frac{I}{wh}$ | Eq. 6 |
|--|--------------------|-------|

Here, j represents the electrical current flux vector, B the magnetic field vector, I the electrical current vector, w the channel width, and h the flow depth. This body force is somewhat analogous to gravity in the case of uniform electric current and magnetic field. A $j \times B$ force term may be added to Eq. 3, resulting in Eq. 7. This additional term has been used previously to predict flow depth changes in a channel due to $j \times B$ forces [3]. The chosen subscripts reflect the resultant equation based on the setup of LMX-U.

| | | |
|--|---|-------|
| | $\frac{\rho g h_0^2}{2} + \frac{j_{0,x} B_z h_0^2}{2} + \rho u^2 h_0 = \frac{\rho g h_1^2}{2} + \frac{j_{1,x} B_z h_1^2}{2} + \rho u^2 h_1$ | Eq. 7 |
|--|---|-------|

An equation similar in form to Eq. 4 may be derived by including the effects of vertically directed Lorentz force in the momentum conservation equation. This process yields Eq. 8, and a new dimensionless number appears that relates $j \times B$ force to gravitational force.

| | | |
|--|---|-------|
| | $\frac{h_1}{h_0} = \frac{-(1 + \gamma_0) + \sqrt{(1 + \gamma_0)^2 + 8Fr^2}}{2}$ | Eq. 8 |
|--|---|-------|

The value γ_0 represents the ratio between vertically (aligned with gravity) directed Lorentz force upstream of the jump and gravitational force. A positive value of gamma implies Lorentz force points in the same direction as gravity, and can be evaluated at a location using Eq. 9 where the subscript \hat{j} indicates the component aligned with gravity by chosen convention.

| | | |
|--|--|-------|
| | $\gamma = \frac{(j \times B)_{\hat{j}}}{\rho g}$ | Eq. 9 |
|--|--|-------|

1.3 Applications to Nuclear Fusion

Liquid metal plasma facing components (LM-PFCs) have been of interest to fusion reactor design due to their ability to actively remove large amounts of heat that solid-state components cannot handle [4]. Fast-flowing LM-PFC concepts rely on the liquid metal to remove heat from the plasma without getting so hot that the liquid metal excessively evaporates. These types of LM-PFC flows are projected to have thickness and flow speed on the order of 0.5-2.0 [cm] and 10 [m/s] respectively [5]. These parameters in Eq. 4 predict a depth change factor of 40 following a hydraulic jump. Such a drastic change in flow depth would be catastrophic in application as the liquid metal would not drain properly, potentially flooding the reactor and causing rapid evaporation.

Of principal concern is whether a hydraulic jump is likely to occur in a thin, fast flowing LM-PFC, and how the addition of magnetic fields and externally injected electric currents may affect the onset of a jump. Thus, the position and depth change of the hydraulic jump in a liquid metal system was studied under various configurations to see how magnetic fields and Lorentz force could be used to suppress and/or delay jumps.

1.4 Previous Work

Free-surface liquid metal channel flows have received attention in past work in the context of fast-flowing LM-PFCs. Amongst the topics of interest, supercritical flow phenomena and hydraulic jumps have been studied [6, 7]. Some research has also been done on hydraulic jumps taking place in highly electrically conductive flows with magnetic fields [8]. Work looking at the ways in which a hydraulic jump is affected by a Lorentz force created from externally injected electric currents and magnetic fields has not been thoroughly studied, and is the main subject of this work.

The importance of having smooth, fast-flow in a liquid metal divertor has been evaluated in the past, and the presence of hydraulic jumps are incompatible with this requirement [9]. Detailed studies have been done to evaluate evaporation in flowing liquid metals, and based on the expected temperature rise that would result from flow changes following a hydraulic jump the evaporation would be far greater than allowable [10].

2. Experimental Overview

The experimental results presented in this paper were obtained using the Liquid Metal eXperiment-Upgrade (LMX-U) test facility at the Princeton Plasma Physics Lab. Galinstan (GalSn eutectic alloy) is used as the working liquid metal as it is liquid at room temperature and non-

toxic. Several works on LMX have been recently published that describe the system in more detail, with the upgraded components described in this work [3, 11].

LMX-U used a 3HP rotary gear pump to circulate the liquid metal. A height-adjustable planar nozzle at the inlet allowed the inlet flow depth and speed to be changed for a given flow rate. Adjusting the height of the inlet nozzle led to a change in the channel flow depth, but for small nozzle heights this depth increased significantly further downstream of the nozzle. This effect is attributed to imperfections in the channel leading to accumulated energy losses as well as channel wetting issues that caused the galinstan to thicken from the edges due to its large surface tension.

The pump and nozzle changes from the original LMX were intended to increase flow rate and decrease the inlet depth, permitting the study of Froude numbers greater than unity. MHD drag was minimized by using acrylic channel walls that acted as electrically insulating boundary conditions [12]. A depiction of the liquid metal loop can be found in Figure 1.

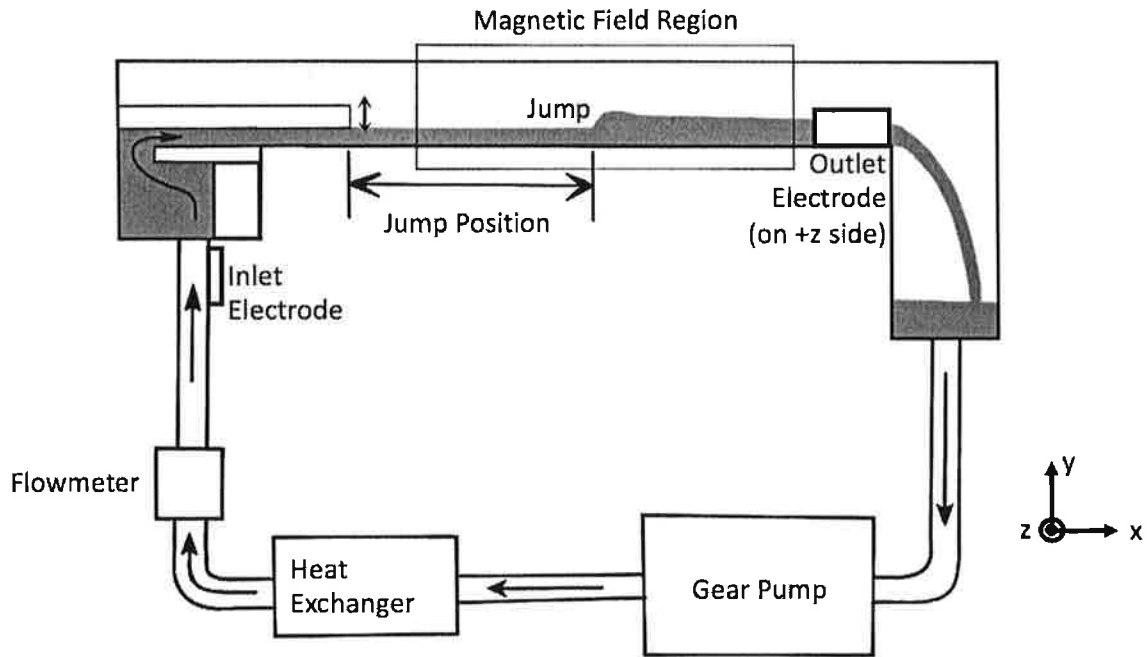


Figure 1: A schematic of the liquid metal loop—LMX-U. Not to scale.

Depth measurements were taken using a laser sheet incident on the surface of the liquid metal that is tracked by a CCD camera. This diagnostic has been used in past work on LMX as a non-intrusive height measurement [3]. The now upgraded sliding laser sheet configuration allows for measurements to be taken at various locations in the channel as both the laser sheet and CCD

camera slide with no relative motion. A schematic of the diagnostic is shown in Figure 2, with a sample imaging of a hydraulic jump shown in Figure 3.

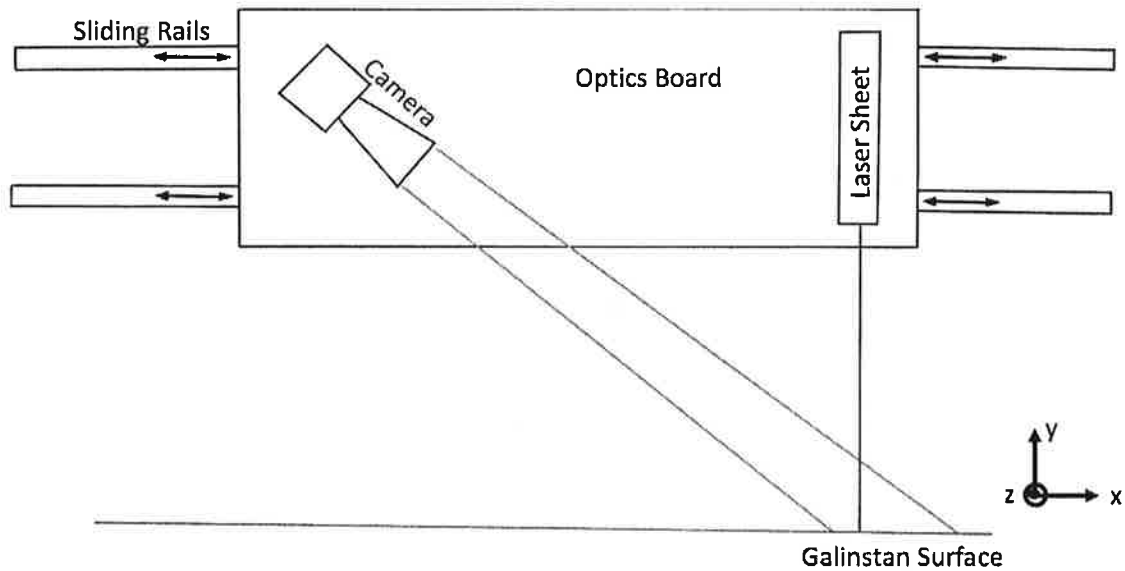


Figure 2: Schematic of the sliding laser sheet setup

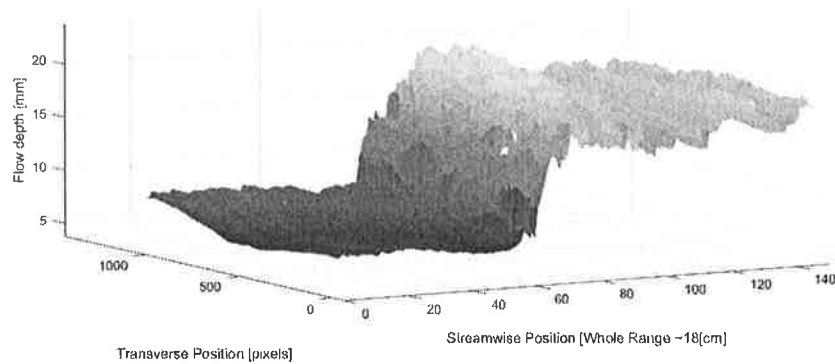


Figure 3: Sample imaging of a hydraulic jump using laser sheet diagnostic.

Flow rates for each experiment were controlled using a variable frequency drive (VFD) with a pump control resolution of one RPM. An Omega FMG96 electromagnetic flowmeter was installed downstream of the pump to verify the flowrate—the flowmeter was factory-certified for less than 1% measurement error at the flowrates used.

The magnet used for LMX-U is also described in past work, and provides a magnetic field up to 0.33 [T] with roughly 4% field strength variation across the width of the test section [3]. A top-down view of the magnet setup is shown in Figure 4, and a view along the channel in Figure 5.

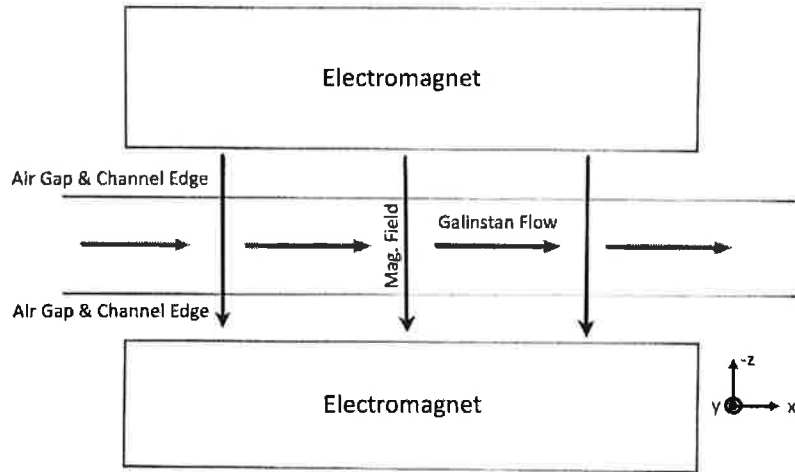


Figure 4: An overhead schematic of the LMX-U electromagnet setup.

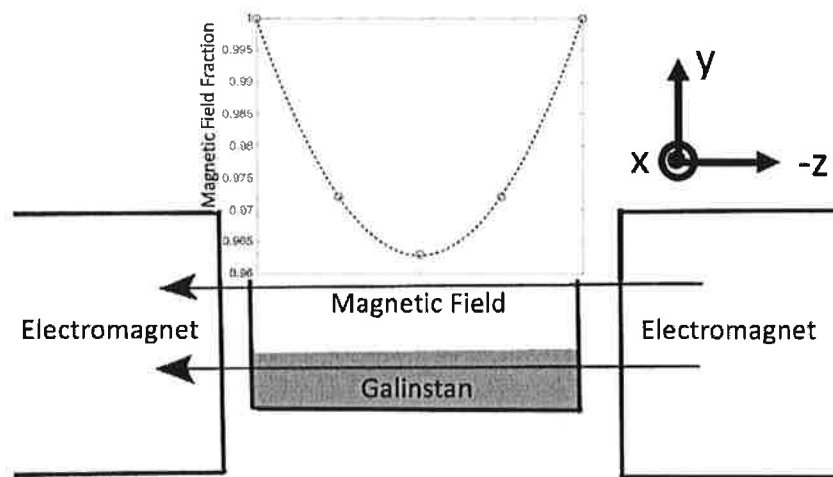


Figure 5: Schematic of magnet strength across channel width, looking down the length of the channel with flow out of the page.

Electrodes located upstream of the channel inlet as well as the outlet allowed for externally injected electric currents up to 140 [A] using a DC power supply. These electrodes can be seen in Figure 1: A schematic of the liquid metal loop—LMX-U.

To reach flows with Froude number greater than one either the flow rate was increased or the flow depth decreased in accordance with Eq. 1. Decreasing flow depth also acted to increase the flow speed as the flow speed is inversely proportional to the depth according to Eq. 2, making flow depth the most impactful variable when trying to raise Froude number.

It is important to note that over time the galinstan oxidized even though LMX was purged of air with Argon gas to avoid oxidization. The system may have had a small air leak, remnant air that couldn't be removed, or even oxygen impurities in the argon used to inert the channel. As the galinstan accumulated oxides the flow characteristics eventually changed, requiring the oxides to be removed. Removal of oxides was done by allowing oxides to collect in the outlet waterfall on LMX as they are less dense than the galinstan, and then unsealing the channel to scrape them off the top layer.

The data presented in each figure were collected during the same "cleaning" such that not enough oxides had accumulated to make significant changes to flow behavior. Due to slight discrepancies in the cleanings the system did not behave identically between cleanings, but this should not pose any major problems in analyzing the data. This effect made large data sets difficult to take, resulting in the number of data points to be limited in a large parameter scan.

3. Hydraulic Jump Control Using Lorentz Force

Previous investigations done with LMX quantified the effect of Lorentz force generated through externally injected electrical currents and magnetic fields on the flow depth [3]. Upon inspection of momentum conservation equations, the depth changes were attributed to essentially increasing/decreasing 'effective' gravity using Lorentz force directed parallel or anti-parallel to gravity.

Galinstan has a large surface tension when compared to other liquids that are traditionally used in hydraulic jump experiments (nearly ten-times that of water), and does not easily wet most conventional materials. The surface tension of galinstan was experimentally measured to be 0.61-0.62 [N/m] using a pendant drop experiment. Other sources have reported galinstan to have a surface tension of 0.533 [N/m], however the amount of oxide on the galinstan surface is observed to change surface tension and [13, 14]. The combination of these two effects causes non-negligible opposition forces to the liquid metal becoming too thin (minimum depth was roughly 6 [mm]). Surface tension is also known to affect the hydraulic jumps, although the effects were not thoroughly investigated in this study [15].

3.1 Jump Position

The tendency for a hydraulic jump to move due to changes in downstream depth is governed by the 'sensitivity'. Jump sensitivity is defined by Eq. 10 [16]:

| | | |
|--|---------------------------------|--------|
| | $S = \frac{\Delta x}{\Delta y}$ | Eq. 10 |
|--|---------------------------------|--------|

where Δx and Δy are changes in hydraulic jump location and flow depth downstream of the jump respectively, as illustrated in Figure 6.

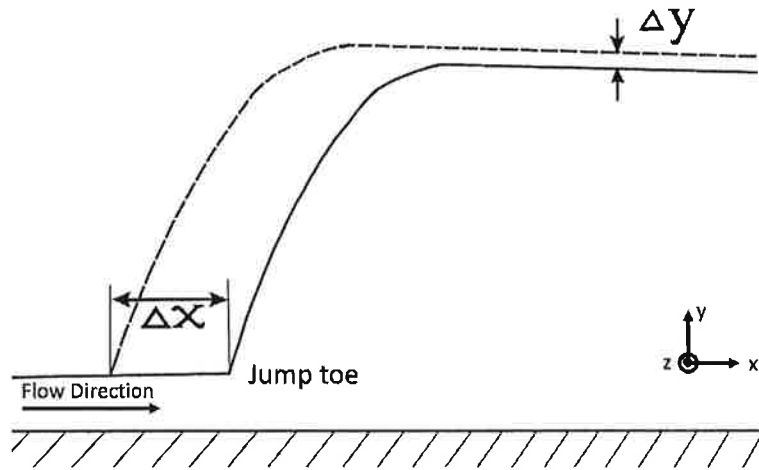


Figure 6: A schematic showing Δx and Δy when calculating the sensitivity of a hydraulic jump—not to scale for jumps observed in LMX-U.

A vertically directed Lorentz force has been shown to alter flow depth in channel flows, and this effect may be used to move a hydraulic jump according to jump sensitivity. One can also expect the jump itself to change in nature due to the depth variation caused by Lorentz force upstream of the jump, but decoupling the two effects is difficult.

3.1.1 Flow Rate Dependence

Before using magnetic fields or electric currents, the jump position versus flow rate was measured with data shown in Figure 7. An exact theory curve cannot be determined due to imperfections and non-wetting fluid behavior in LMX-U. However, Eq. 11 is a known relation between flow rate and jump position and is shown scaled by a constant for best fit [17].

| | | |
|--|--|--------|
| | $x_p \propto \left(\frac{Q}{w}\right)^{5/3} \nu^{-1} g^{-1/3}$ | Eq. 11 |
|--|--|--------|

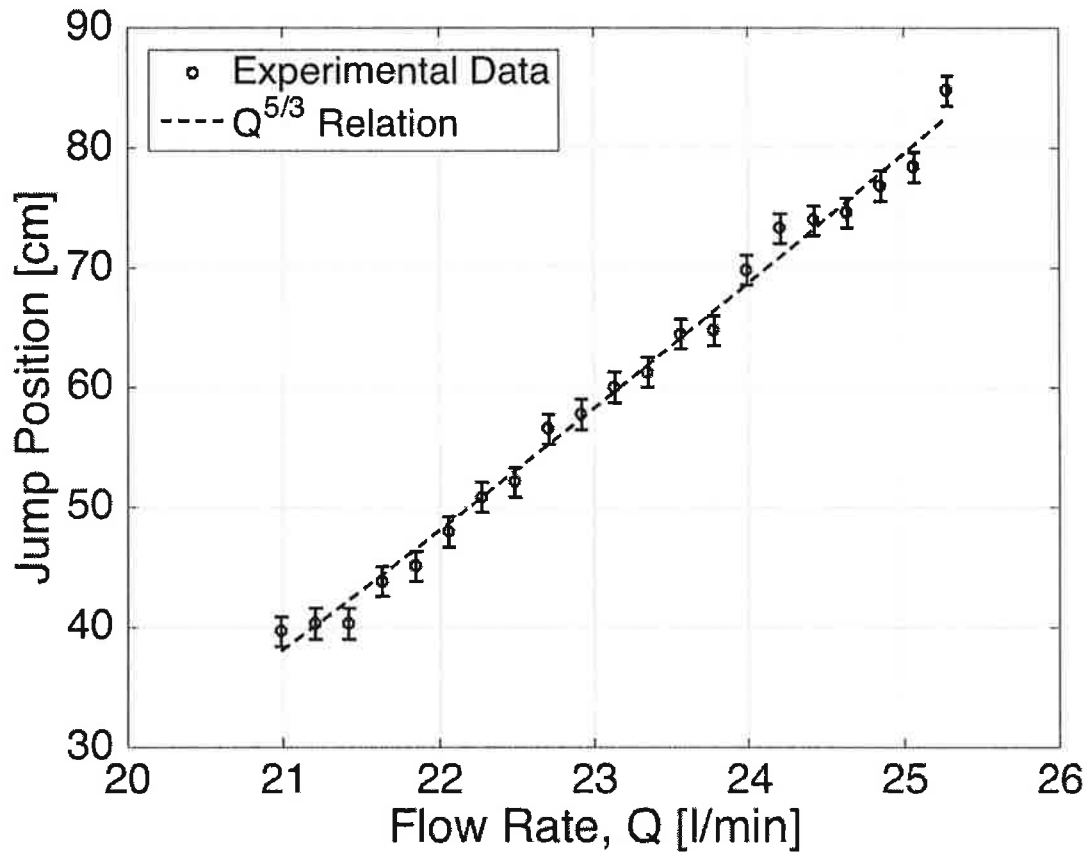


Figure 7: Hydraulic jump location versus flow rate in channel. Jump position represents how far downstream from the nozzle outlet the jump occurred.

3.1.2 Magnetic Field Dependence

Jump location was measured for a variety of steady-state magnetic field strengths ranging from 0-0.15 [T]. The nozzle height was kept fixed at 3 [mm] as it was in the jump position versus flow rate experiment, and flow rate was fixed at 22 [l/min]. Even with the nozzle height at 3 [mm] the flow visibly increased in depth far upstream of the jump, leading to upstream jump depths greater than 8 [mm]. Data for position as a function of magnetic field is shown in Figure 8. Due to the relatively short length of LMX-U channel the jump could not be moved further with stronger magnetic fields.

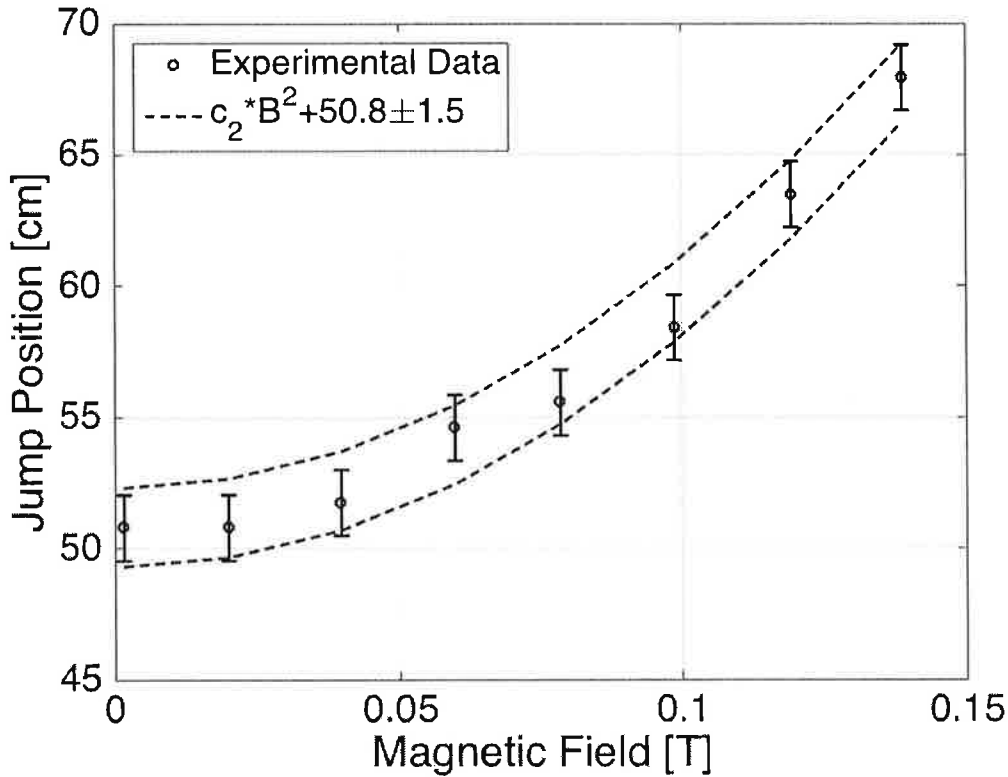


Figure 8: Jump position versus magnetic field. Error bars represent uncertainty in the jump position, while dashed blue lines are an envelope for a quadratic fit.

Because the data set shown in Figure 8 was taken during a separate cleaning of the channel and galinstan, the zero magnetic field data point here did not necessarily line up with the position shown in Figure 7, despite the same nozzle and flow rate settings. When increasing the magnetic field to beyond 0.15[T], the hydraulic jump became less clear and at high enough magnetic fields (approaching 0.3[T]) the jump was suppressed entirely within the channel length.

A definitive relation explaining this curve was not determined. One explanation is a potential link to a reduction in “effective” viscosity caused by the magnetic field—thus causing the jump position to move downstream as suggested in Eq. 11. Past work on LMX show a roughly $1/B$ dependence in “effective” viscosity as an explanation for the effect magnetic fields had on vortex shedding downstream of a cylinder [18]. This change in “effective” viscosity could cause a nearly linear dependence of jump position on magnetic field using Eq. 11.

A second explanation is more generally attributed to how magnetic fields have effects on turbulent structures in conductive flows. The MHD drag appears as a volume force in the momentum equation, given by Eq. 12. This force is directed opposite to fluid motion, hence the name MHD drag.

| | | |
|--|--|--------|
| | $F_D = \sigma(\mathbf{u} \times \mathbf{B}) \times \mathbf{B}$ | Eq. 12 |
|--|--|--------|

The ability of this force to restrict perturbations perpendicular to magnetic field has been shown to anisotropically reduce flow turbulence [19, 20]. The observed hydraulic jump position trend may be attributed to this force suppressing flow perturbations. However, other experiments have shown drag in the bulk flow direction to cause an upstream trend on jump position, opposite to the trends observed in this work. The differences can be mostly attributed to changes in experimental setup and magnetic field direction [21]. Because LMX has an electrically insulating duct the drag associated with bulk flow is reduced, but velocity perturbations are still damped.

3.1.3 $j \times B$ Force Dependence

Externally injected electrical currents were also added to several of the magnetic field configuration. Figure 9 shows a parameter scan of $j \times B$ force resulting from varying electrical current for three different magnetic fields. These three data sets were collected in the same channel cleaning to minimize differences in flow conditions between the different magnetic field settings.

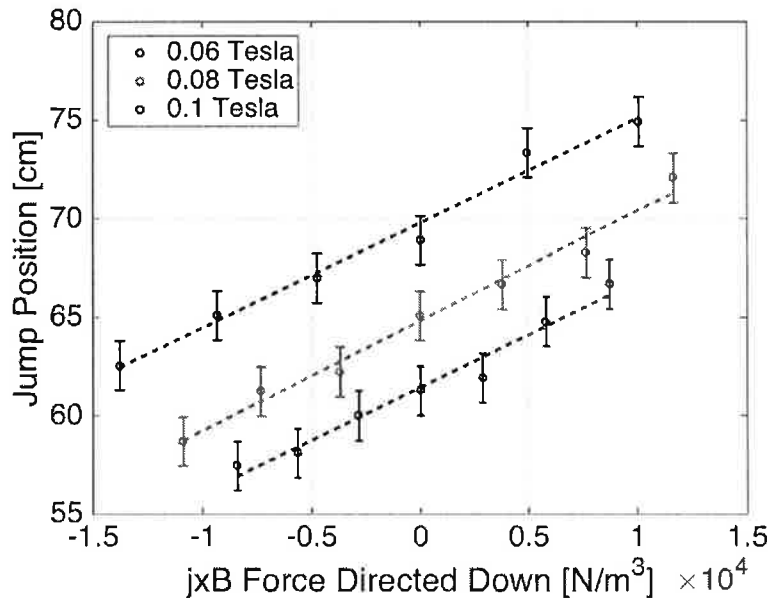


Figure 9: Length-wise position of hydraulic jump versus $j \times B$ force directed downwards (i.e., a negative value implies the force is directed upwards against gravity). Three different magnetic fields were tested on the same cleaning of the system, each exhibited the same linear trend within 2% with $j \times B$.

As jxB force changed, the flow depth experienced depth changes that have been investigated in past work on LMX. Compared to gravitational force this is a relatively narrow regime of jxB force, and values of γ_0 stay below 0.25 in magnitude. Based on past results and measurements, the depth change in this regime is close to linear with respect to changes in jxB [3]. For the experimental case presented in Figure 9 the depth change downstream of the jump over the jxB domain was measured to be 0.9 [mm], compared to the position shift of 125 [mm]. A jump sensitivity of approximately 140 can then be calculated according to Eq. 10. The theoretical sensitivity of the jump in LMX is plotted in Figure 10. The curve is described by Eq. 19, and derived using Eq. 8 rather than Eq. 4 in combination with Eq. 13 through Eq. 18 [16]. For the presented case, the channel slope i is zero, leading to several terms dropping out in the final form of the equation.

| | | |
|--|--|--------|
| | $\Delta Y = \Delta D_2 + i(\Delta X - \Delta L)$ | Eq. 13 |
|--|--|--------|

| | | |
|--|---|--------|
| | $\frac{1}{S} = \frac{\partial D_2}{\partial X} \left(\frac{\partial D_2}{\partial D_1} + i \left(\frac{\partial X}{\partial D_1} - \frac{\partial L}{\partial D_1} \right) \right)$ | Eq. 14 |
|--|---|--------|

| | | |
|--|---------------------------|--------|
| | $\frac{L}{D_1} = 9Fr - 9$ | Eq. 15 |
|--|---------------------------|--------|

| | | |
|--|--|--------|
| | $\frac{\partial L}{\partial D_1} = -4.5Fr - 9$ | Eq. 16 |
|--|--|--------|

| | | |
|--|---|--------|
| | $\frac{\partial D_2}{\partial D_1} = \frac{2(1 + \gamma) - 8Fr^2 - 2\sqrt{(\gamma + 1)^2 + 8Fr^2}}{4\sqrt{(\gamma + 1)^2 + 8Fr^2}}$ | Eq. 17 |
|--|---|--------|

| | | |
|--|--|--------|
| | $\frac{\partial D_1}{\partial x} = \frac{i - j}{Fr^2 - 1}$ | Eq. 18 |
|--|--|--------|

| | | |
|--|--|--------|
| | $S = \left(\frac{Fr^2 - 1}{j} \right) \left(\frac{2\sqrt{(\gamma_0 + 1)^2 + 8Fr^2}}{\sqrt{(\gamma_0 + 1)^2 + 8Fr^2} - (1 + \gamma_0) + 4Fr^2} \right)$ | Eq. 19 |
|--|--|--------|

The variable j is a friction coefficient. This is solved for numerically using a form of the Colebrook-White equation shown in Eq. 20 over a range of depths while holding the other variables constant, the Froude number increasing as depth decreases according to Eq. 1 [22].

| | | |
|--|--|--------|
| | $\frac{\left(\frac{Q}{w^2}\right) \sqrt{1+2\gamma}}{4\left(\frac{h_0}{w}\right)^{\frac{3}{2}} \sqrt{2gj}} = \log_{10} \left(\frac{3.187 \sqrt{2gj} \left(\frac{D^{\frac{3}{2}}}{\nu}\right)}{\left(1 + \frac{2h_0}{w}\right)^{\frac{3}{2}}}\right)$ | Eq. 20 |
|--|--|--------|

The experimentally calculated sensitivity was subject to large error, but fell close to the calculated value. Froude number varied from roughly 1.4 to 2 across experiments where sensitivity calculations remain relatively constant.

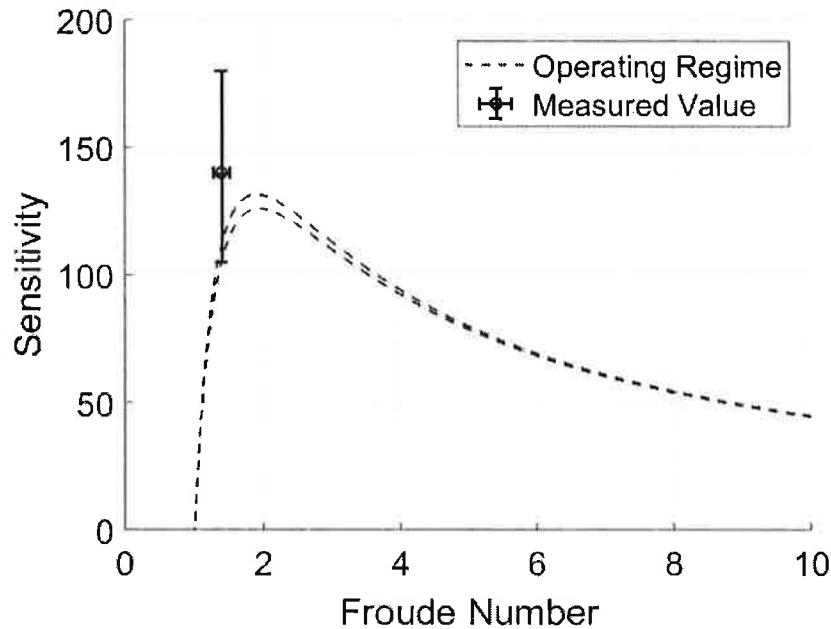


Figure 10: Sensitivity calculated with $Q = 5.9$ [GPM], $w = 0.109$ [m], $B = 0.1$ [T], $I = +135$ [A] (upper bound), $I = -135$ (lower bound), Froude number is varied through changes in depth upstream of the jump. The error bar results from uncertainty in depth measurements.

Predicting the initial position of a hydraulic jump is done using a backwater curve in many applications. The LMX channel bed had several localized imperfections upstream of the jump locations that could not be practically accounted for in addition to non-traditional flow behavior of the galinstan.

3.2 Jump Depth Change

The depth ratio across the hydraulic jump was measured with changing jxB force. Measurements of h_0 were taken to be the depth leading up to the jump, while measurements of h_1 were taken at the peak depth. For each flow condition the sliding laser sheet was swept over the jump approximately ten times, each providing a depth measurement upstream and downstream of the jump.

Measurements of h_1 were more variant than measurements of h_0 due to the turbulence created following the jump. Using Eq. 8, the expected h_1/h_0 value was calculated and compared to the measured value for various jxB force. The trend of h_1/h_0 versus jxB is shown in Figure 11, while the comparison between data and calculation is shown in Figure 12.

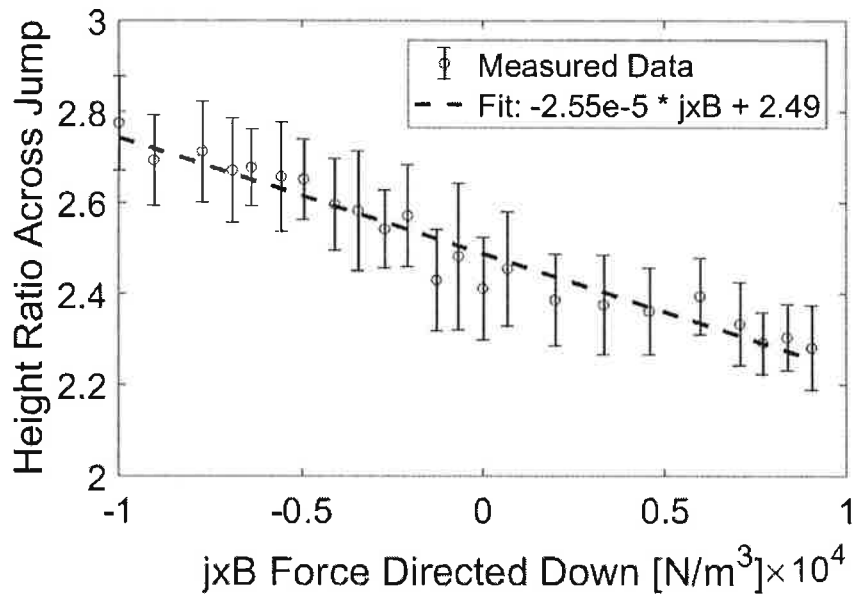


Figure 11: Measured values of h_1/h_0 versus jxB , one standard deviation bars shown.

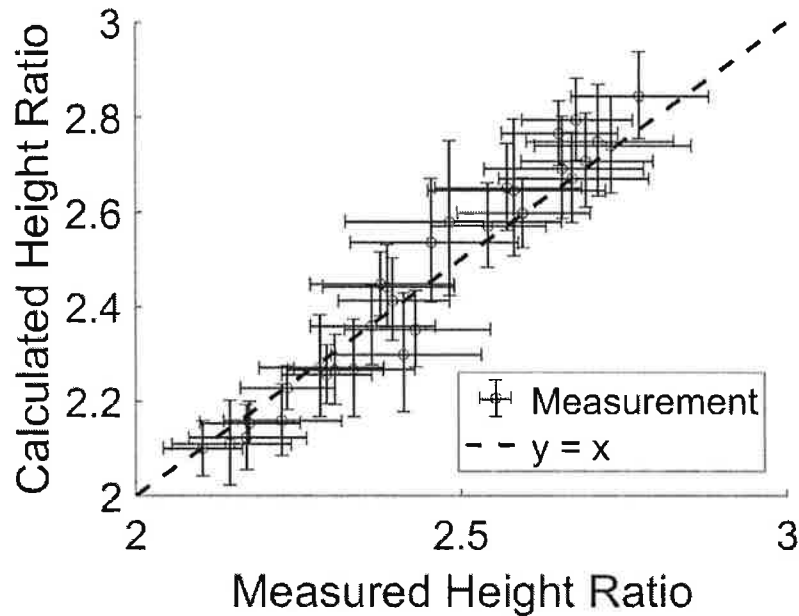


Figure 12: Comparison of calculated and measured height ratio, one standard deviation bars shown. Calculated height ratio errors result from uncertainty in the upstream depth measurement. Data was taken while the system was operating at a flow rate of 28.7 [l/min], magnetic field 0.082 [T] and electrical current varying from +/- 140 [A].

A 3 [mm] high weir was installed at the end of the channel during this experiment to measure height ratio. This was done in order to more strictly enforce the subcritical condition at the end of the channel so data could be taken at higher flow rates. Froude number varied between 1.7 and 1.9 during these measurements as the upstream depth underwent small changes.

4. Discussion

Hydraulic jumps pose a serious problem to fast-flowing liquid metal film PFCs by causing splashing, and deceleration of flow that may lead to evaporation. The results presented show how $j \times B$ force effects liquid metal hydraulic jumps and ways to prevent jumps from occurring.

The jump position change compared to $j \times B$ force for different magnetic field configurations is consistent, suggesting that the effects of $j \times B$ force are independent of the effects of a given magnetic field strength. As $j \times B$ force was increased to even higher values directed downwards not shown in the plots (greater than $1.5e4$ [N/m³]), the hydraulic jump changed in nature from a weak jump to an undular jump such that a jump position and depth ratio could not be taken and compared to results from the weak jump.

When using a magnetic field as high as 0.3 [T] there was no jump at all, and the flow remained supercritical for the entire channel length. This is a positive result for liquid metals in a reactor setting as the transverse magnetic fields are 1 - 6 [T], having a stronger suppression effect. It is

difficult to make a direct comparison however because a fast-flowing liquid metal divertor will most likely flow radially outwards, leading to circular hydraulic jumps which are different in nature [23].

5. Conclusions & Future Work

This experiment clearly demonstrated the control of hydraulic jump location and depth ratio in a channel using electromagnetic forces. The qualitative observations of $j \times B$ force and magnetic fields causing hydraulic jumps to fade also suggests the ability to stop hydraulic jump from occurring all together. These results build upon previous studies of hydraulic jump, and provide additional insight into the effects of $j \times B$ on a channel flow. Radial jump configurations applicable to fusion reactors are of great interest, and it is hoped that these experiments may be performed in a radial flow configuration.

6. Acknowledgments

The authors would like to thank K. Caspary, D. Dudd, E. Gilson and Y. E. Yu for their assistance and insights throughout these experiments.

The research described was funded through the Laboratory Directed Research and Development Program (LDRD) at Princeton Plasma Physics Laboratory, a U.S. Department of Energy National Lab operated by Princeton University.

Digital data for this paper can be found at:

<http://arks.princeton.edu/ark:/88435/dsp01x920g025r>

7. Works Cited

- [1] J. B. Bélanger, "Essai sur la Solution Numérique de quelques Problèmes Relatifs au Mouvement Permanent des Eaux Courantes," Carilian-Goeury, Paris, 1828.
- [2] W. H. Hager, Energy Dissipators and Hydraulic Jump, Dordrecht: Springer Netherlands, 1992.
- [3] M. G. Hvasta, E. Kolemen, A. Fisher and H. Ji, "Demonstrating Electromagnetic Control of Free-Surface, Liquid-Metal Flows Relevant to Fusion Reactors," *Nuclear Fusion*, vol. 58, no. 1, 2017.

- [4] M. A. Abdou, N. B. Morley, A. Y. Ying, S. Smolentsev and P. Calderoni, "Overview of Fusion Blanket R&D in the US Over the Last Decade," *Nuclear Engineering and Technology*, vol. 37, no. 5, pp. 401-422, 2005.
- [5] M. A. Abdou, "On the Exploration of Innovative Concepts for Fusion Chamber Technology," *Fusion Eng. and Design*, vol. 54, pp. 181-247, 2001.
- [6] N. B. Morley, *Numerical and experimental modeling of liquid metal thin film flows in a quasi-coplanar magnetic field*, Los Angeles: UCLA, 1994.
- [7] M. Narula, A. Ying, M. A. Abdou and R. Moreau, "Liquid Metal Free Surface Flow Through a Non-Uniform Magnetic Field: An Experimental Study," in *Conference on Fundamental and Applied MHD*, 2005.
- [8] M. Narula, A. Ying and M. A. Abdou, "A Study of Liquid Metal Film Flow Under Fusion Relevant Magnetic Fields," *Fusion Science and Technology*, vol. 47, pp. 564-568, 2005.
- [9] R. E. Nygren, T. D. Rognlien, T. D. Rensink, S. S. Smolentsev, M. Z. Youssef, M. E. Sawan, B. J. Merrill, C. Eberle, P. J. Fogarty, B. E. Nelson, D. K. Sze and D. Majeski, "A fusion reactor design with a liquid first wall and divertor," *Fusion Engineering and Design*, vol. 72, no. 1-3, pp. 181-221, 2004.
- [10] R. W. Moir, "Liquid First Walls for Magnetic Fusion Energy Configurations," *Nuclear Fusion*, vol. 37, no. 4, pp. 557-566, 1997.
- [11] M. G. Hvasta, E. Kolemen and A. Fisher, "Application of IR imaging for free-surface velocity measurement in liquid-metal systems," *Rev. Sci. Instrum.*, 2017.
- [12] S. Malang and L. Buhler, "MHD Pressure Drop in Duct with Imperfectly Insulating Coatings," Argonne National Laboratory, Lemont, IL, 1994.
- [13] N. B. Morley and J. Burris, "The MTOR LM-MHD Facility, and Preliminary Experimental Investigation of Thin Layer, Liquid Metal Flow in a 1/R Toroidal Magnetic Field," *Fusion Sci. Technol.*, vol. 44, pp. 74-78, 2003.
- [14] H. Ji, W. Fox, D. Pace and H. L. Rappaport, "Study of Small-Amplitude Magnetohydrodynamic Surface Waves on Liquid Metal," *Physics of Plasmas*, vol. 12, no. 1, p. 012102, 2005.
- [15] R. I. Bowles and F. T. Smith, "The standing hydraulic jump: theory, computations and comparisons with experiments," *J. Fluid Mech.*, vol. 242, pp. 145-168, 1992.
- [16] E. Wilson, "Location of the Hydraulic Jump in Open Rectangular Channels," *The Engineer*, vol. 223, pp. 145-149, 1967.
- [17] J. K. Bhattacharjee and A. K. Ray, "Hydraulic Jump," *Journal of Physics: Conference Series*, vol. 319, no. 1, p. 012003, 2011.
- [18] J. R. Rhoads, E. M. Edlund and H. Ji, "Effects of Magnetic Field on the Turbulent Wake of a Cylinder in Free-Surface Magnetohydrodynamic Channel Flow," *J. Fluid Mech.*, vol. 742, pp. 446-465, 2014.
- [19] J. R. Rhoads, *Magnetohydrodynamics and Heat Transfer in a Free-Surface, Flowing Liquid Metal Experiment*, Princeton: Princeton University, 2013.

- [20] A. Y. Ying, M. A. Abdou, N. Morley, T. Sketchley, R. Woolley, J. Burris, R. Kaita, P. Fogarty, H. Huang, X. Lao and M. Narula, "Exploratory studies of flowing liquid metal divertor options for fusion-relevant magnetic fields in the MTOR facility," *Fusion Engineering and Design*, vol. 72, pp. 35-62, 2004.
- [21] H. B. Löfgren and H. O. Åkerstedt, "Electromagnetic Braking of the Flow of a Liquid Metal With a Free Surface," *Fluid Dynamics Research*, vol. 23, no. 1, pp. 1-25, 1998.
- [22] E. S. Crump, "Flow of Fluids in Conduits and Open Channels," *Proc. I. Civ. Eng.*, vol. 5, no. 4, pp. 522-526, 1956.
- [23] T. Bohr, C. Ellegaard, A. E. Hansen and A. Haaning, "Hydraulic jumps, flow separation and wave breaking: An experimental study," *Physica B: Condensd Matter*, vol. 228, no. 1-2, pp. 1-10, 1996.